International Journal of Microwave and Wireless Technologies

cambridge.org/mrf

Miniaturized triple-band monopole antenna loaded with a via-less MTM for 3G, WIMAX, and WLAN applications

Mohammadsadegh Kasmaei[1], Ehsan Zareian-Jahromi[1], Raheleh Basiri[1] and Valiollah Mashayekhi[2]

[1]Department of Electrical and Electronic Engineering, Shiraz University of Technology, Shiraz, Iran and
[2]Department of Electrical Engineering, Shahrood University of Technology, Shahrood, Iran

Research Paper

Cite this article: Kasmaei M, Zareian-Jahromi E, Basiri R, Mashayekhi V (2022). Miniaturized triple-band monopole antenna loaded with a via-less MTM for 3G, WIMAX, and WLAN applications. *International Journal of Microwave and Wireless Technologies* **14**, 601–608. https://doi.org/10.1017/S1759078721000702

Received: 4 December 2020
Revised: 13 April 2021
Accepted: 13 April 2021
First published online: 11 May 2021

Keywords:
Metamaterial (MTMs); 3G; WLAN; WiMAX; antenna bandwidth.

Author for correspondence:
Valiollah Mashayekhi,
E-mail: vmashayekhi@shahroodut.ac.ir

Abstract

In this paper, a tri-band metamaterial (MTM) loaded compact monopole antenna is proposed. In the first step of design procedure, a rectangular monopole antenna is improved by replacing the corresponding rectangular patch with a ring resonator. As a result, the first obtained operating frequency is decreased from 2.95 to 2.46 GHz. Then, this operating frequency is reduced to 2.02 GHz utilizing an MTM geometry in the antenna structure. The geometry parameters of the proposed antenna are optimized to provide the applicability for 3G, WLAN, and WiMAX applications. The impedance bandwidths of 600, 1080, and 220 MHz are obtained at 2.02–2.62, 3.48–4.56, and 5.12–5.34 GHz, respectively. Moreover, the equivalent circuit of the proposed antenna has been extracted. The proposed equivalent circuit model is validated through a comparison with corresponding simulation results. The proposed antenna is compact, low profile, via-less, and provides easy fabrication. Considering the first resonance frequency, a compactness of 32% is achieved in comparison to the corresponding unloaded monopole antenna.

Introduction

Modern wireless communication systems including Wireless Local Area Network (WLAN) and Worldwide interoperability for Microwave Access (WiMAX) are heading toward designing the characteristics of compact size, multiband, greater impedance bandwidth (super band antenna), and omnidirectional pattern [1–3]. Designing antenna structures considering the above-mentioned features is regarded as a major challenge [2–4].

The metamaterials (MTMs) are used in various structures to provide multiband and multifunctional demanded features as well as increased bandwidth property [5, 6]. The adaption of composite right/left-handed (CRLH) MTMs or simply MTM unit cells can lead to improved antennas such as enhanced leaky-wave antennas [7], multifunctional antennas [8], and resonator-type antennas [9, 10].

Low cost, low profile, and multiband operating capability features of monopole planar structures make them a good candidate for WLAN and WiMAX applications. The negative order resonances and reduced resonance frequencies of MTM microstrip patch antennas result in size reduction and antenna miniaturization [11, 12]. Moreover, the multifrequency properties of MTM loaded antennas make them adequate for multiband applications [8, 13].

In this paper, a low profile CRLH loaded monopole antenna is proposed for 3G, 2.4 GHz WLAN, and 2.55 GHz WiMAX (2.02–2.62 GHz), 3.5 GHz WiMAX (3.48–4.56 GHz), and 5.2 GHz WLAN (5.12–5.34 GHz) applications. To reduce the fabrication cost, a via-free CRLH unit cell is taken into account. In comparison with a simple unloaded antenna, the utilized MTM loading leads to distinct frequency bands with wide frequency bandwidths. A full-wave simulator based upon the finite-element method solutions of Maxwell's equations is used in design procedure. Also, the equivalence circuit model of the proposed structure is proposed [12–14]. The proposed MTM loaded antenna is fabricated whereas corresponding measurements are compared with simulation results to ensure the enhanced performance characteristics.

The paper is organized as follows. In section "Antenna design", the antenna design procedure is briefly described. In section "Equivalent circuit", equivalent circuit of the proposed antenna has been extracted. The current distributions of the proposed antenna are discussed in section "Current distribution". In section "Experimental results", the measurement results of the proposed antenna are presented whereas conclusion remarks are presented in section "Conclusion".

CAMBRIDGE
UNIVERSITY PRESS

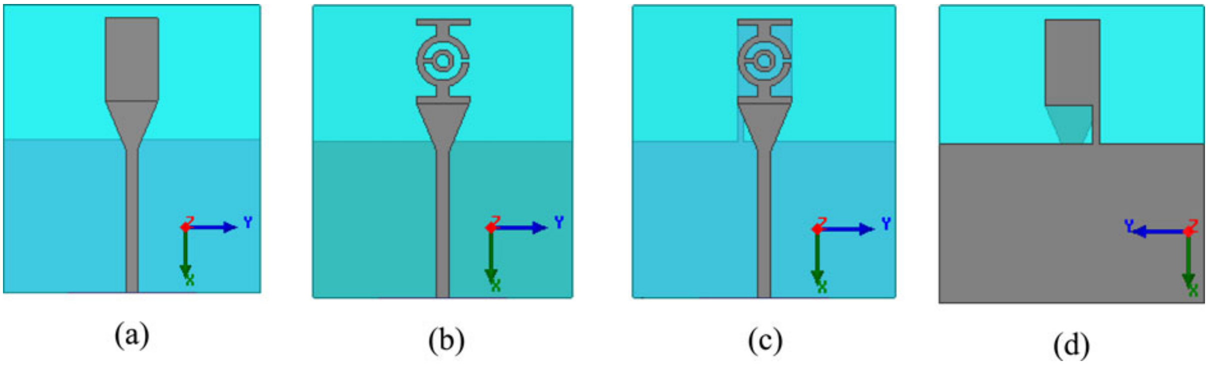

Fig. 1. Design evolution for the proposed tri-band MTM antenna; (a) unloaded monopole antenna; (b) replacing patch with ring resonator; proposed tri-band antenna with single-cell MTM loading: (c) top view and (d) bottom view.

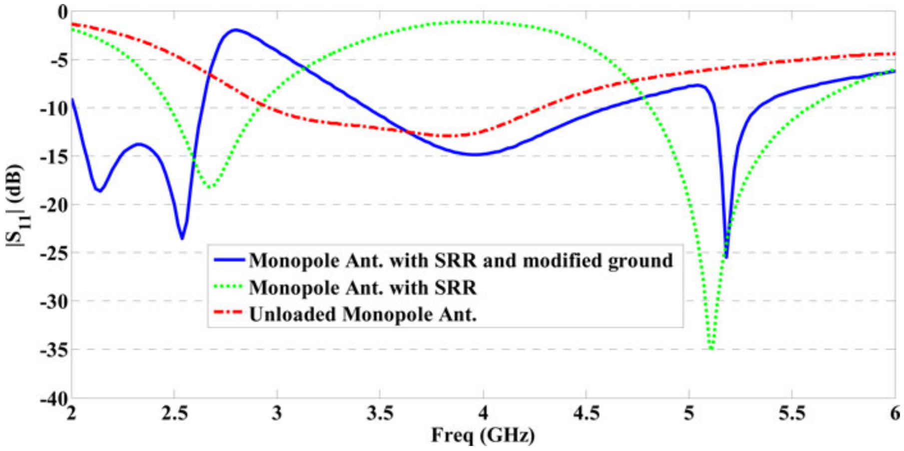

Fig. 2. Simulated return loss of different antenna configurations in Fig. 1.

Antenna design

The various design schematic evolutions of the proposed tri-band antenna are shown in Fig. 1. All simulations and fabrications are based on the utilization of an FR4 substrate with a thickness of $h = 1$ mm, relative electric permittivity of $\varepsilon_r = 4.4$, and $\tan\delta = 0.02$. The design procedure is detailed as follows.

Unloaded monopole antenna

First, an unloaded monopole antenna is investigated to provide a primary structure to which the next modified antennas are compared. The monopole structure is demonstrated in Fig. 1(a) in which the feed line is separated by a slot from the radiating patch. The corresponding reflection coefficient is investigated in Fig. 2 resulting in $|S11| < -10$ dB at 2.95–4.32 GHz with a resonant frequency of 3.64 GHz.

Dual-band monopole antenna with a ring resonator

The first modified antenna is obtained by replacing the radiating patch in Fig. 1(a) with a ring resonator demonstrated in Fig. 1(b). Two distinct frequency bandwidths of about 430 and 750 MHz with corresponding resonance frequencies of around 2.68 and 5.11 GHz are obtained. Therefore, dual-band operation is achieved together with 26% antenna geometry compactness.

Proposed tri-band monopole antenna with MTM loading

In order to obtain a tri-band antenna and achieve more compactness, the final configuration is proposed in Figs 1(c) and 1(d) based on MTM loading. According to Fig. 2, the proposed antenna operates around 2.32 GHz (2.02–2.62 GHz), 4.02 GHz (3.48–4.56 GHz), and 5.23 GHz (5.12–5.34 GHz). In addition to tri-band performance achievement, a compactness of 32% is achieved considering the first resonance frequency.

The geometry parameters of the proposed MTM loaded monopole antenna is demonstrated in Fig. 3. The full size of the introduced monopole antenna is $\mathrm{L} \times \mathrm{W} \times \mathrm{h}\ \mathrm{mm}^3$ whereas the overall size of the radiating patch is $\mathrm{Lr} \times \mathrm{Wr}\ \mathrm{mm}^2$. According to Fig. 3(a), a slot separates the feed line from the ring resonator as the main radiator. Moreover, the embedded MTM structure is realized through an inductive thin strip connecting the rectangular patch to the ground plane.

These geometry parameters are optimized to achieve demanded applicability for 3G, WLAN, and WiMAX applications. Moreover, the best geometry compactness is also considered. The finalized geometry parameters of the proposed MTM loaded antenna are listed in Table 1.

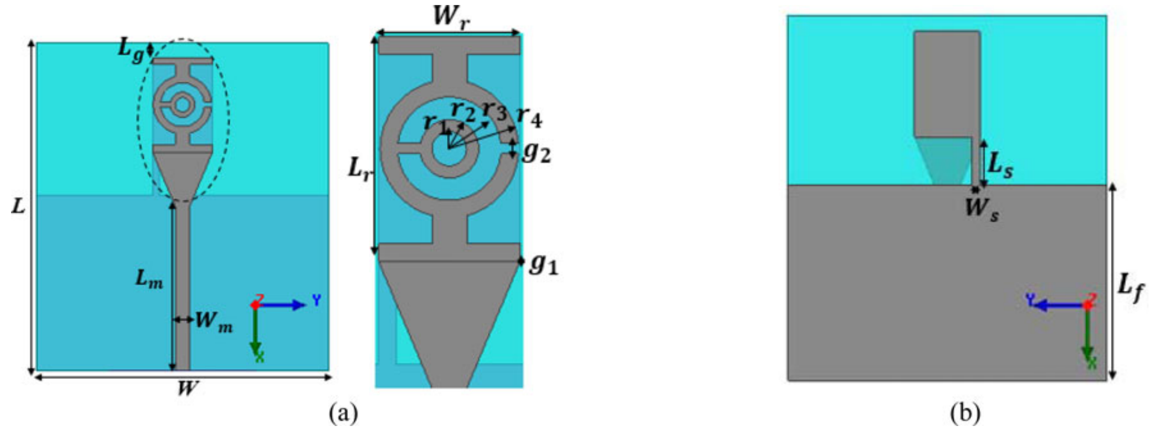

Fig. 3. Geometry parameters of the proposed MTM loaded monopole antenna: (a) top view and (b) bottom view.

Table 1. Dimensions of the proposed MTM antenna in Fig. 3

Parameters	Values (mm)	Parameters	Values (mm)
L	45	W_r	8.2
L_m	22.5	r_1	1
L_g	2	r_2	2
L_r	13	r_3	3
L_s	1.5	r_4	4
W	40	g_1	0.05
W_m	1.9	g_2	0.5
W_s	4.1		

Table 2. Values of circuit elements in Fig. 4

Parameters	Values	Parameters	Values
L_1	2.438 nH	C_4	9.426 PF
L_2	0.647 nH	θ_1	365°
L_3	0.348 nH	θ_2	390°
C_1	0.648 PF	Z_1	421.6 Ω
C_2	6.02 PF	Z_2	32.08 Ω
C_3	0.348 PF	R_1	29.92 Ω

Equivalent circuit

Here, the equivalent circuit model of the proposed via-free antenna is investigated [12, 13, 15, 16]. According to Fig. 4, a CRLH structure is obtained. Corresponding to Fig. 3, the strip located at the antenna base is defined by L1 and R1 whereas C1 is considered to model the capacitance between this inductive strip and ground plane. Moreover, the antenna radiation loss is modeled with a resistance merged in R1. The tapered strip at the end part of feed line is modeled through a transmission line defined by Z1 and θ1. The embedded slot between tapered strip line and ring resonator results in a left-handed series capacitance, C2, whereas the ring resonator is modeled as a parallel tank circuit including inductance L3 and capacitance C3.

The capacitance between the SRR and the rectangular patch beneath it at the ground plane is modeled by C4. Moreover, the mentioned rectangular patch at the ground plane is defined by a transmission line represented by Z2 and θ2. Finally, L2 is yielded from the resulting current flow on an inductive thin strip connecting mentioned rectangular patch to the ground plane. The circuit elements C2, C3, C4, and L2 provide the left-hand property of the proposed antenna.

The corresponding values of these circuit elements are optimized to achieve the best reflection coefficient in comparison to simulations. The finalized extracted values for these circuit elements are detailed in Table 2. The reflection coefficient of the introduced antenna is demonstrated in Fig. 5. A good agreement between simulations performed by HFSS software and those obtained by the present circuit model can be found in Fig. 5. The observed differences can be justified as the disability of the

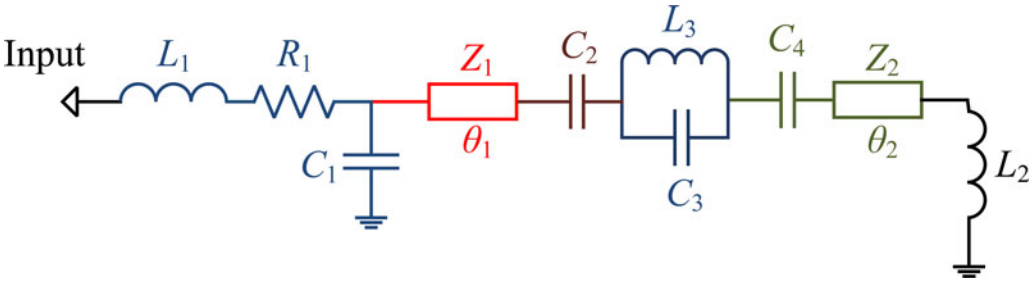

Fig. 4. Equivalent circuit model of the proposed antenna in Fig. 3.

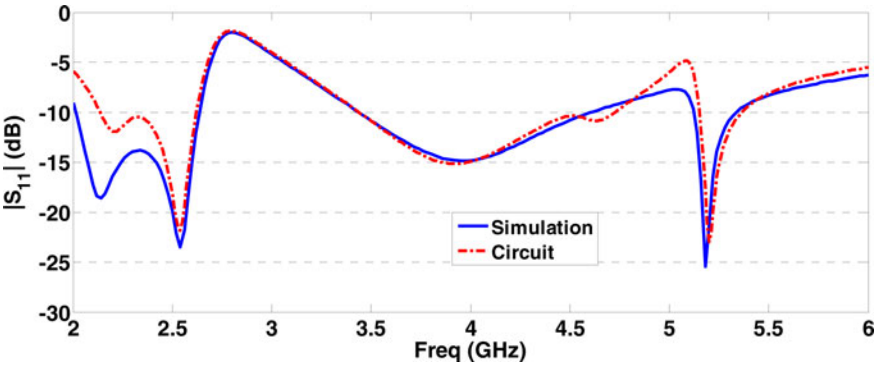

Fig. 5. Return loss corresponding to extracted equivalent circuit in Fig. 4.

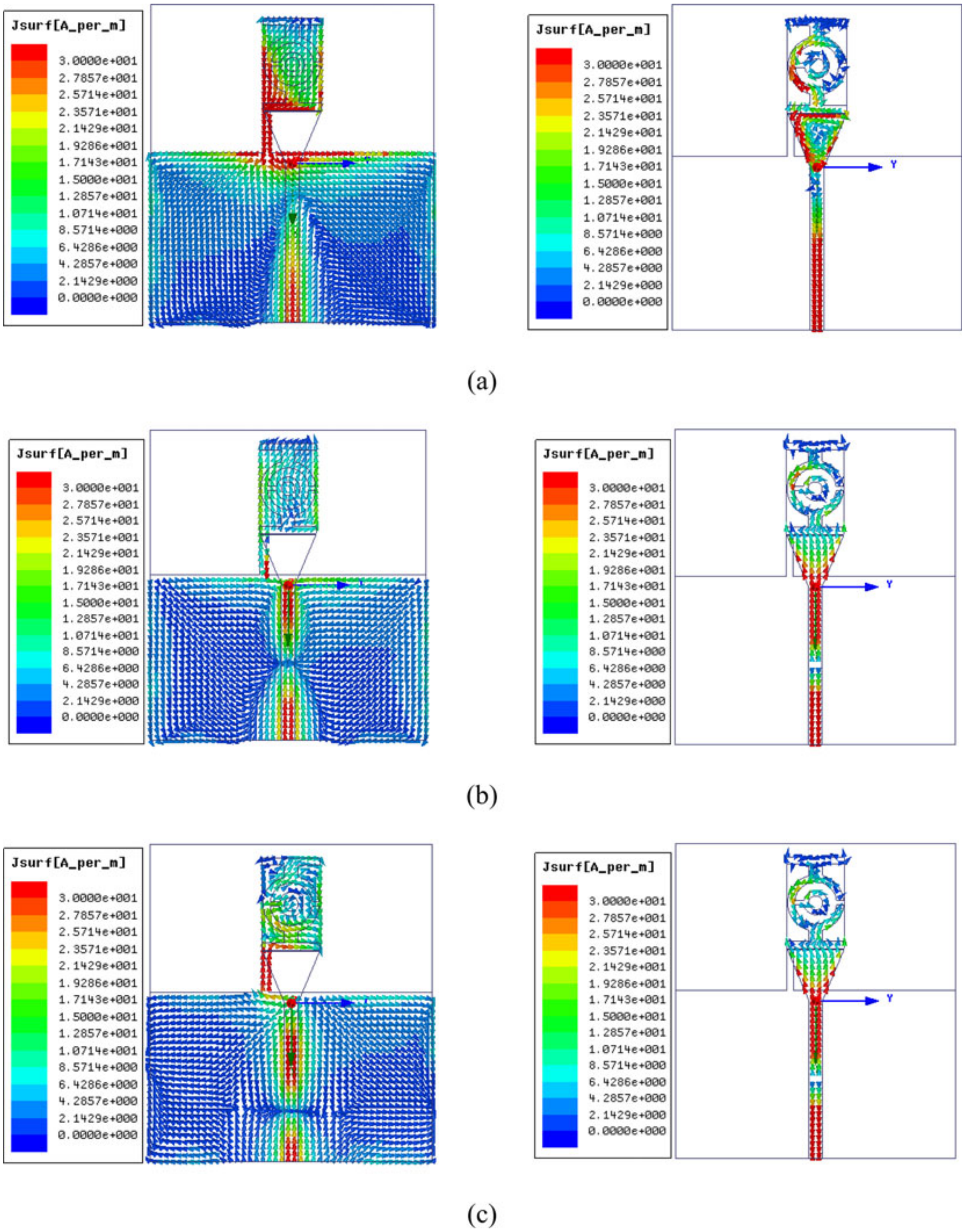

Fig. 6. Current distribution on the proposed antenna in Fig. 3 for three resonant frequencies (a) 2.12 GHz, (b) 4.12 GHz, and (c) 5.16 GHz.

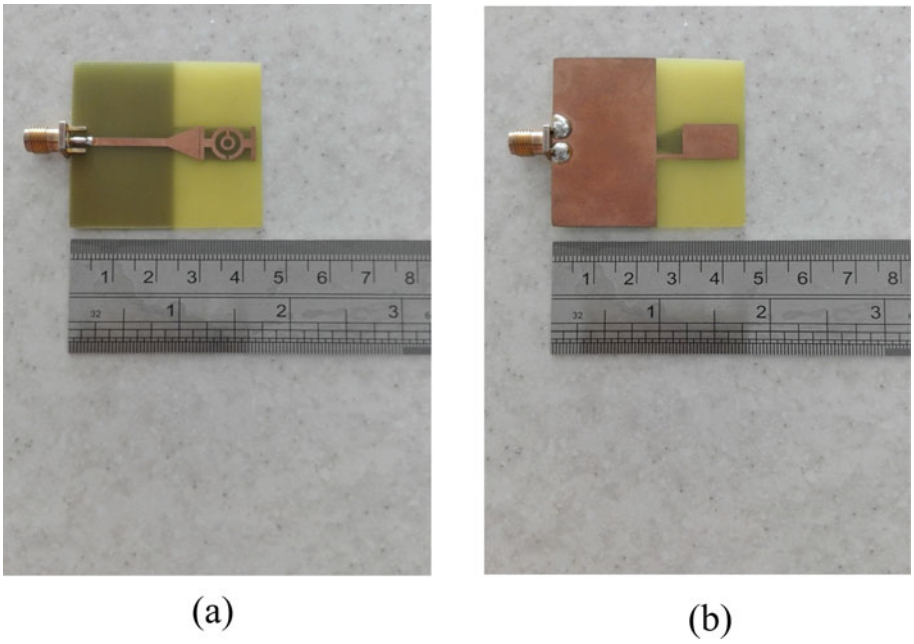

Fig. 7. Fabricated antenna in Fig. 3 with a soldered SMA connector; (a) top view and (b) bottom view.

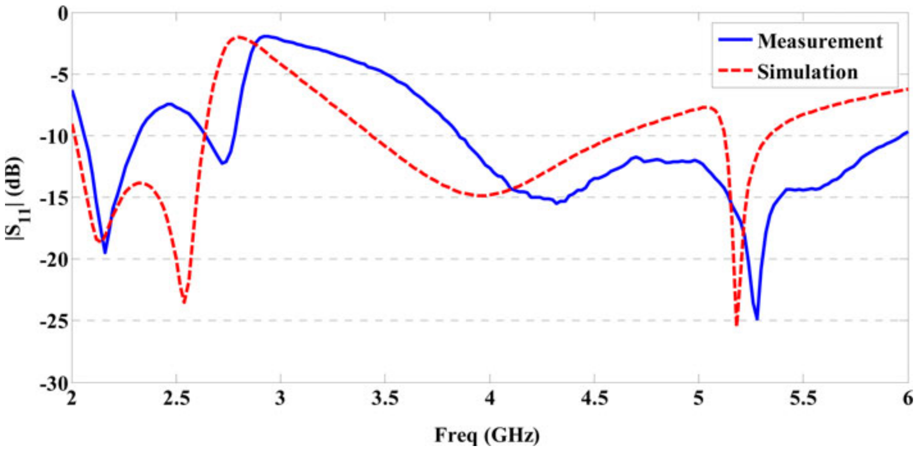

Fig. 8. Measured and simulated reflection coefficients of the proposed antenna in Fig. 3.

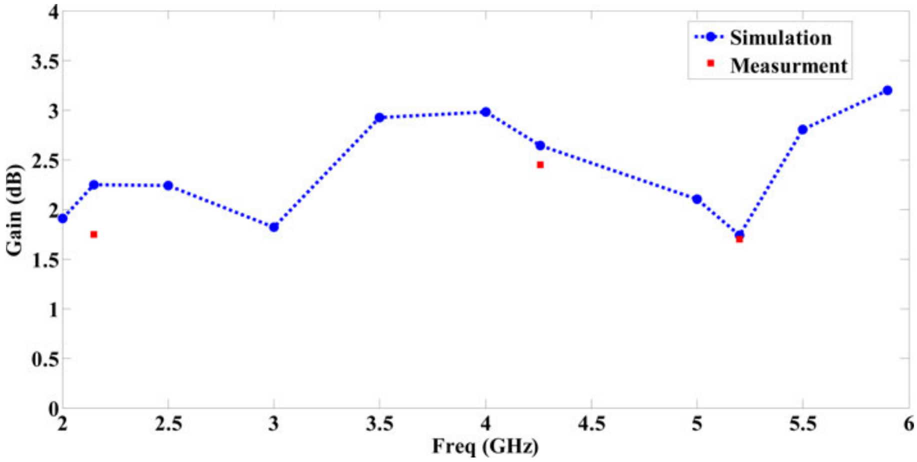

Fig. 9. Measured and simulated maximum gain of the proposed antenna.

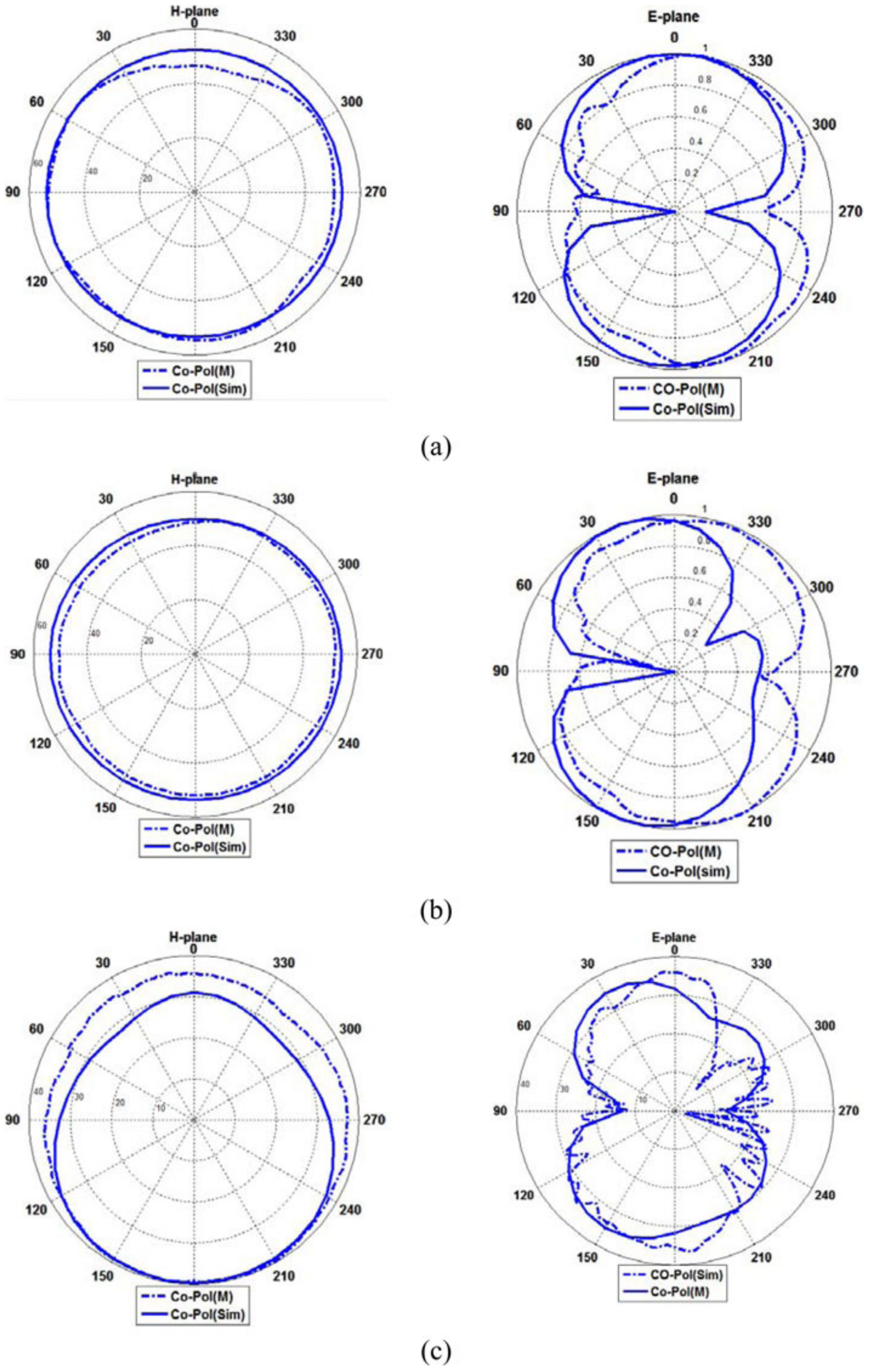

(a)

(b)

(c)

Fig. 10. Radiation patterns of the proposed antenna in Fig. 3 at E- and H-planes considering (a) 2.15 GHz, (b) 4.26 GHz, and (c) 5.28 GHz.

circuit model for considering antenna radiation and simplified couplings and losses presented in Fig. 4.

Current distribution

Current distributions on the proposed antenna at three resonant frequencies, 2.12, 4.12, and 5.16 GHz are demonstrated in Fig. 6. It is known that left-hand property overcomes right-hand feature at low frequencies in MTM structures. The beneficial effect of the inclusion of the left-handed structure is observed at 2.12 GHz. The inductive thin strip and embedded slot corresponding to L2 and C2, respectively, are mainly involved according to Fig. 6(a).

Moreover, the proposed antenna behaves as a CRLH structure at higher frequencies of 4.12 and 5.16 GHz, which is in accordance with current distributions demonstrated in Figs 6(b) and 6(c). According to Fig. 6, the main surface currents are along the *x*-axis representing *x*-directed dipole radiating elements. Therefore, a dipole-like radiation pattern is expected.

Experimental results

The proposed MTM-loaded tri-band monopole antenna is fabricated on an FR4 substrate with a relative electric permittivity of

Table 3. A comparison between the proposed antenna and previously reported similar works

Ref.	Dimensions (mm^3)	First resonant frequency (GHz)	BW (MHz)	Peak gain (dB)	3G	WLAN	WIMAX	Via process
[12]	30 × 22 × 1.5	3.55	3840	–	–	5.2 5.8	3.5	Required
[17]	40 × 40 × 7	2.40	120 1400	1.4 5.1	–	2.4 5.2	5.5 5.8	Not required
[18]	65 × 65 × 6	2.28	270 750	5 6	–	2.4 5.2	5.5	Required
[19]	50 × 50 × 3.17	3.27	100	0.8	–	–	3.5	Required
[20]	180 × 90 × 1.6	2.53	700 700	5 6	–	2.4 5.2	2.5 5.5	Required
[21]	40 × 40 × 1.6	3.2	1380	3.5	–	–	2.5 3.5	Not required
Proposed antenna	45 × 40 × 1	2.02	620 1600 200	2.23 2.81 1.91	2.1	2.4 5.2	2.5 3.5	Not required

4.4 together with a loss tangent of 0.02 and a thickness of 1 mm (Fig. 7). Simulated and measured reflection coefficients are plotted in Fig. 8. A good agreement is observed between measured and simulation results. The differences between measured and simulated results are due to losses of the feeding network and utilized FR4 substrate.

Moreover, a comparison between measured and simulated maximum gain of the proposed antenna is shown in Fig. 9. The measured gain values are about 1.7, 2.45, and 1.75 dB at 2.15, 4.26, and 5.28 GHz, respectively. It is noted that these frequencies represent $|S11|$ measurement resonances in Fig. 8.

Variation of simulated and measured normalized far-field radiation patterns in yz-plane (H-plane) and xz-plane (E-plane) considering 2.15, 4.26, and 5.28 GHz is demonstrated in Fig. 10. As expected, the proposed antenna exhibits a dipolar pattern at E-plane and near omnidirectional pattern at the corresponding H-plane.

Table 3 summarizes the proposed antenna parameters compared with various antenna configurations reported in [12, 17–21]. The provided investigation confirms the efficiency of the designed antenna structure. Utilizing the MTM in the proposed antenna reduces the first resonant frequency and improves corresponding bandwidth. Moreover, a reasonable gain and low profile structure are achieved as well as via-less property of the proposed antenna results in easy and low-cost fabrication.

Conclusion

A tri-band compact monopole antenna is proposed for 3G, WiMAX, and WLAN applications. The antenna consists of a small monopole antenna loaded with a single via-free CRLH TL unit cell. Additionally, the antenna exhibits a measured 10 dB return-loss bandwidth at 2.02–2.62, 3.48–4.56, and 5.12–5.34 GHz. The main features of the proposed antenna are achieved compactness, low profile property, via-less structure, and easy integration with other microwave circuits. A 32% antenna geometry compactness is achieved in comparison to the corresponding unloaded monopole antenna. The simulation and measurement results have been investigated to evaluate the performance of the introduced antenna. Moreover, the corresponding equivalent circuit has been extracted. The validity of the proposed equivalent circuit model is investigated using a comparison with corresponding simulation results.

References

1. **Balanis CA** (2005) Microstrip antennas. *Antenna Theory: Analysis and Design* **3**, 811–882.
2. **Huang H, Liu Y, Zhang S and Gong S** (2015) Multiband metamaterial-loaded monopole antenna for WLAN/WiMAX applications. *IEEE Antennas and Wireless Propagation Letters* **14**, 662–665.
3. **Krishna DD, Gopikrishna M, Aanandan C, Mohanan P and Vasudevan K** (2009) Compact wideband Koch fractal printed slot antenna. *IET Microwaves, Antennas & Propagation* **3**, 782–789.
4. **Moosazadeh M and Kharkovsky S** (2014) Compact and small planar monopole antenna with symmetrical L-and U-shaped slots for WLAN/WiMAX applications. *IEEE Antennas and Wireless Propagation Letters* **13**, 388–391.
5. **Nourbakhsh M, Zareian-Jahromi E and Basiri R** (2019) Ultra-wideband terahertz metamaterial absorber based on Snowflake Koch Fractal dielectric loaded graphene. *Optics Express* **27**, 32958–32969.
6. **Nemat-Abad HM, Zareian-Jahromi E and Basiri R** (2019) Design and equivalent circuit model extraction of a third-order band-pass frequency selective surface filter for terahertz applications. *Engineering Science and Technology, an International Journal* **22**, 862–868.
7. **Jackson DR, Caloz C and Itoh T** (2012) Leaky-wave antennas. *Proceedings of the IEEE* **100**, 2194–2206.
8. **Zhu C, Li T, Li K, Su Z-J, Wang X, Zhai H-Q, Li L and Liang C-H** (2015) Electrically small metamaterial-inspired tri-band antenna with meta-mode. *IEEE Antennas and Wireless Propagation Letters* **14**, 1738–1741.
9. **Ha J, Kwon K, Lee Y and Choi J** (2012) Hybrid mode wideband patch antenna loaded with a planar metamaterial unit cell. *IEEE Transactions on Antennas and Propagation* **60**, 1143–1147.
10. **Amani N and Jafargholi A** (2015) Zeroth-order and TM10 modes in one-unit cell CRLH mushroom resonator. *IEEE Antennas and Wireless Propagation Letters* **14**, 1396–1399.
11. **Dong Y, Toyao H and Itoh T** (2011) Compact circularly-polarized patch antenna loaded with metamaterial structures. *IEEE Transactions on Antennas and Propagation* **59**, 4329–4333.
12. **Antoniades MA and Eleftheriades GV** (2009) A broadband dual-mode monopole antenna using NRI-TL metamaterial loading. *IEEE Antennas and Wireless Propagation Letters* **8**, 258–261.
13. **Zhu J, Antoniades MA and Eleftheriades GV** (2010) A compact tri-band monopole antenna with single-cell metamaterial loading. *IEEE Transactions on Antennas and Propagation* **58**, 1031–1038.
14. **Caloz C and Itoh T** (2005) *Electromagnetic Metamaterials: Transmission Line Theory and Microwave Applications*. USA: John Wiley & Sons.
15. **Jamilan S, Antoniades MA, Nourinia J and Azarmanesh MN** (2015) A directivity-band-dependent triple-band and wideband dual-polarized

monopole antenna loaded with a via-free CRLH unit cell. *IEEE Antennas and Wireless Propagation Letters* **14**, 855–858.

16. **Baena JD, Bonache J, Martín F, Sillero RM, Falcone F, Lopetegi T, Laso MA, Garcia-Garcia J, Gil I, Portillo MF and Sorolla M** (2005) Equivalent-circuit models for split-ring resonators and complementary split-ring resonators coupled to planar transmission lines. *IEEE Transactions on Microwave Theory and Techniques* **53**, 1451–1461.
17. **Kim T-H and Park D-C** (2005) Compact dual-band antenna with double L-slits for WLAN operations. *IEEE Antennas and Wireless Propagation Letters* **4**, 249–252.
18. **Liang Z, Liu J, Li Y and Long Y** (2016) A dual-frequency broadband design of coupled-fed stacked microstrip monopolar patch antenna for WLAN applications. *IEEE Antennas and Wireless Propagation Letters* **15**, 1289–1292.
19. **Zhu J and Eleftheriades GV** (2009) A compact transmission-line metamaterial antenna with extended bandwidth. *IEEE Antennas and Wireless Propagation Letters* **8**, 295–298.
20. **Rezvani M and Zehforoosh Y** (2018) A dual-band multiple-input multiple-output microstrip antenna with metamaterial structure for LTE and WLAN applications. *AEU-International Journal of Electronics and Communications* **93**, 277–282.
21. **Varamini G, Keshtkar A, Daryasafar N and Naser-Moghadasi M** (2018) Microstrip Sierpinski fractal carpet for slot antenna with metamaterial loads for dual-band wireless application. *AEU-International Journal of Electronics and Communications* **84**, 93–99.

Mohammadsadegh Kasmaei received his B.S. degree in electrical engineering from the University of Birjand, Birjand, Iran, in 2015, and his M.S. degree in telecommunications from the Shiraz University of Technology, Shiraz, Iran, in 2017. His current research interests include antenna design and metamaterials.

Ehsan Zareian-Jahromi received his B.S. and M.S. degrees in electrical engineering from the University of Tehran, Tehran, Iran, in 2005 and 2008, respectively, and his Ph.D. degree in telecommunications from the Amirkabir University of Technology, Tehran, Iran, in 2013. From July to December 2012, he was a Visiting Scientist at the University of Bologna, Bologna, Italy. He is currently an Assistant Professor of electrical engineering with the Shiraz University of Technology, Shiraz, Iran. His current research interests include antenna design, metamaterials, periodic structures, electromagnetic compatibility, and numerical methods in electromagnetics.

Raheleh Basiri received her B.S., M.S., and Ph.D. degrees in communication engineering from Shiraz University, Shiraz, Iran, in 2005, 2008, and 2015, respectively. Since 2015 she has been with the Electrical Engineering Department, Shiraz University of Technology, where she is now an assistant Professor. Her research interests include numerical methods in electromagnetic theory, microwave and terahertz devices and antenna, and graphene and metamaterials.

Valiollah Mashayekhi was born in Tehran, Iran, in 1983. He received his B.S. degree in electrical engineering from the Shahrood University of Technology, Shahrood, Iran, in 2006, and the M.S. and Ph.D. degrees in telecommunications from the Amirkabir University of Technology, Tehran, Iran, in 2010 and 2017, respectively. He is currently an Assistant Professor of electrical engineering with the Shahrood University of Technology, Shahrood, Iran. His current research interests include antenna design, metamaterials, numerical methods in electromagnetics, electromagnetic compatibility, and power system transients with particular reference to LEMP interaction with electrical networks and grounding systems.